3상 PWM AC-AC 부스트 컨버터의 DSP 기반 전류 프로그램 제어

論 文
55B-1-5

DSP-based Current Programmed Control of Three Phase PWM AC-AC Boost Converter

崔 南 燮† · 李 玉 龍*
(Nam-Sup Choi · Yulong Li)

Abstract - In this paper, a new scheme of current programmed control for three phase PWM AC-AC converter is presented. Compared to duty-ratio voltage control, current programmed control has several advantages such as reduction of system order, inherent current protection and robust output. By considering only the magnitude components, a similar scheme in the DC-DC converter can be extended to the three phase PWM AC-AC converter. The proposed current programmed control will be well adopted into various converter topologies though three phase PWM AC-AC boost converter is treated as an example. The converter analysis is carried out by applying the vector DQ transformation to obtain physical insight into the converter operation and to establish some important characteristic equations for control purpose. The experiment results show the validity of the proposed scheme.

Key Words : Current Programmed Control, PWM AC-AC Boost Converter, DQ transform, DSP

Nomenclature

$\mathbf{x}$, $\mathbf{X}$	matrix notation
$\boldsymbol{x}$	complex variable or complex number
$\mathbf{x}^T$	transpose of a matrix
$\boldsymbol{x}^*$	conjugate of a complex variable
$\mathbf{x}_{\psi abc}$	matrix composed of three phase quantities, $[x_{\psi a}, x_{\psi b}, x_{\psi c}]^T$
$\mathbf{x}_{\psi qdo}$	matrix composed of quantities obtained by DQ transform, $[x_{\psi q}, x_{\psi d}, x_{\psi o}]^T$
x_d	d-axis component in DQ transform
x_q	q-axis component in DQ transform
j	complex number $\sqrt{-1}$
s	Laplacian variable
d	duty ratio of Q_1, Q_3, Q_5 switches
V_s	rms value of line-to-line source voltage
ω	angular frequency of source voltage
f	frequency of source voltage in Hz
L	inductance of input side inductors
r	parasitic resistance of input side inductors
C	capacitance of output capacitors
$i_{L,mag}$	magnitude of three phase inductor current
$v_{o,mag}$	magnitude of three phase output voltage
v_{ref}	reference magnitude of three phase output voltage
$i_{L\mu}$	μ phase inductor current (μ = a, b, c)
$v_{s\mu}$	source voltage of μ phase (μ = a, b, c)
$v_{t\mu}$	node voltage at $i_{L\mu}$ current injecting point (μ = a, b, c)
$v_{o\mu}$	μ phase output voltage (μ = a, b, c)
$i_{g\mu}$	current flowing into μ phase output side (μ = a, b, c)
$\boldsymbol{v}_s$	complex voltage obtained by DQ transform of $v_{s\mu}$ (μ = a, b, c), i.e., $\boldsymbol{v}_s = v_{sd} + j\, v_{sq}$
$\boldsymbol{i}_L$	complex current obtained by DQ transform of $i_{L\mu}$ (μ = a, b, c), i.e., $\boldsymbol{i}_L = i_{Ld} + j\, i_{Lq}$
$\boldsymbol{v}_t$	complex voltage obtained by DQ transform of $v_{t\mu}$ (μ = a, b, c), i.e., $\boldsymbol{v}_t = v_{td} + j\, v_{tq}$
$\boldsymbol{i}_g$	complex current obtained by DQ transform of $i_{g\mu}$ (μ = a, b, c), i.e., $\boldsymbol{i}_g = i_{gd} + j\, i_{gq}$
$\boldsymbol{v}_o$	complex voltage obtained by DQ transform of $v_{o\mu}$ (μ = a, b, c), i.e., $\boldsymbol{v}_o = v_{od} + j\, v_{oq}$
D	duty ratio d at operating point
$\boldsymbol{V}_s$	DC value of $\boldsymbol{v}_s$ at operating point
$\boldsymbol{I}_L$	DC value of $\boldsymbol{i}_L$ at operating point
$\boldsymbol{V}_o$	DC value of $\boldsymbol{v}_o$ at operating point
$\hat{d}$	the amount of perturbation of duty ratio d
$\hat{\boldsymbol{i}}_L$	the amount of perturbation of $\boldsymbol{i}_L$
$\hat{\boldsymbol{v}}_o$	the amount of perturbation of $\boldsymbol{v}_o$
$\hat{\boldsymbol{i}}_c$	the amount of perturbation of reference or command current for inductor current $\boldsymbol{i}_L$

† 교신저자, 正 會 員 : 麗水大 工大 電子通信電氣工學部 副教授 · 工博
E-mail : nschoi@yosu.ac.kr
* 學生會員 : 麗水大 工大 電子通信電氣工學部 碩士課程
接受日字 : 2005年 8月 12日
最終完了 : 2005年 12月 6日

1. Introduction

Current programmed control has been widely used in switching converters. Numerous attempts have been made to characterize this control scheme with small signal models. Current programmed DC-DC converter has been dealt with in many papers[1-4]. In [1] and [2], complete analysis and discussion are presented for the three basic converters. In [3], a continuous-time current-mode control model together with sampling accuracy is discussed. In [4], a unified model is established for a current programmed converter.

The current programmed control for AC-AC switching converters, however, has rarely been investigated. This paper proposes a practical current programmed control scheme for AC-AC switching converters.

By considering only the magnitude components, a similar scheme as in the DC-DC converter can be extended to AC-AC case. The actual inductor current magnitude follows the current command through the inner current control loop.

The proposed current programmed control scheme has several advantages over conventional duty cycle control method. By processing the switching control signal with the current programmed controller, the small-signal control-to-output transfer function contains one less pole than that of duty cycle control, so the system order will be reduced. Such reduced system order may lead to easier controller design. Also, as the current programmed controller makes use of the sensed the inductor current information during normal converter operation, transistor failures due to excessive switch current can be prevented simply by setting the current reference value. Hence, inherent current protection is realized.

The proposed current programmed control will be well adopted into various converter topologies such as buck, boost, buck-boost, etc[5]. The three phase PWM AC-AC boost converter is treated as an example in this paper. Basic converter analysis is carried out by performing vector DQ transformation[6], thus some important characteristic relations are obtained for control purpose.

Finally, an experimental setup is made and the experiment results support the design and analysis.

2. System Description

2.1 Operation Principle

Fig. 1(a) shows the conventional duty cycle control diagram of the three phase PWM AC-AC converter. The output AC voltage is sensed and compared with a reference value to generate an error signal, which will be processed by a compensator. The duty control signal is made according to the compensator output.

Fig. 1(b) illustrates the proposed current programmed control diagram of the three phase PWM AC-AC converter. As seen in Fig. 1(b), the three phase AC output voltages will be sensed so as to produce the corresponding output voltage magnitude $v_{o,mag}$ instantly. This voltage magnitude is compared with a reference value to generate the voltage error signal v_e. The error signal is then processed by a PI compensator to form the inductor current magnitude command i_c. The sensed inductor current magnitude component $i_{L,mag}$ is compared with i_c to make the current error signal i_e. Then this current error signal is processed by a PID controller to update the duty ratio, and the PWM switching signal is made by comparing the duty with a triangular waveform with the switching frequency. Thus the actual inductor current magnitude follows the current command through the inner current control loop.

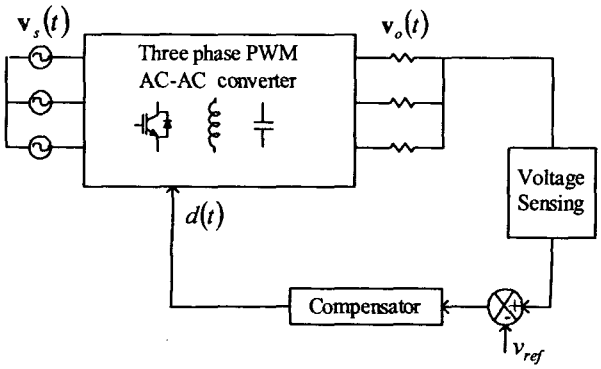

(a) Duty cycle voltage control

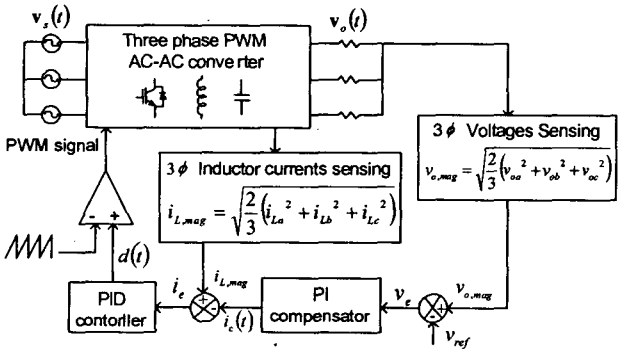

(b) Proposed current programmed control

Fig. 1 Control block diagram of the PWM AC-AC converter

By processing the switching control signal with the current programmed controller, the small-signal control-to-output transfer function $\hat{v}_o(s)/\hat{i}_c(s)$ contains one less pole than $\hat{v}_o(s)/\hat{d}(s)$, so the system order will be reduced. Also, since the inductor current is directly controlled, the behavior is somewhat like the controlled

current source, which will consequently make robust output. Moreover, the current magnitude is limited by the current command, thus inherent over-current protection will be realized.

2.2 Converter Circuit

Fig. 2 shows the three-phase PWM Boost AC-AC converter. As seen in Fig. 2, the system requires six IGBTs. In Fig. 2, r represents parasitic resistance of L. Also, d means the duty ratio of Q_1, Q_3 and Q_5 where they turn on or off in the way of simultaneous switching. Similarly, Q_2, Q_4 and Q_6 turn on or off simultaneously. Therefore, it should be noted that the system under analysis has only one control variable, d.

The source voltages with angular speed, ω are assumed ideal and balanced and are given as follows

$$\mathbf{v}_{sabc}=\begin{bmatrix}v_{sa}\\ v_{sb}\\ v_{sc}\end{bmatrix}=\sqrt{\frac{2}{3}}\cdot V_s\begin{bmatrix}\sin(\omega t)\\ \sin(\omega t-2\pi/3)\\ \sin(\omega t+2\pi/3)\end{bmatrix} \tag{1}$$

where V_s is the rms line-to-line AC source voltage.

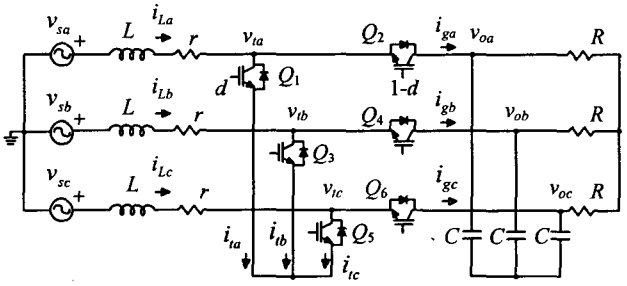

Fig. 2 Three phase PWM AC-AC boost converter

3. Converter Analysis

3.1 Vector DQ Transformation

A vector DQ transformation of three phase quantities $\mathbf{x}_{yabc}$ into a complex vector $\boldsymbol{x}_y$ is defined as

$$\mathbf{x}_{yqdo}=\mathbf{K}\mathbf{x}_{yabc}=[x_{yq}\ \ x_{yd}\ \ x_{yo}]^T \tag{2}$$

$$\mathrm{K}=\sqrt{\frac{2}{3}}\begin{bmatrix}\cos(\omega t) & \cos\left(\omega t-\frac{2\pi}{3}\right) & \cos\left(\omega t+\frac{2\pi}{3}\right)\\ \sin(\omega t) & \sin\left(\omega t-\frac{2\pi}{3}\right) & \sin\left(\omega t+\frac{2\pi}{3}\right)\\ 1/\sqrt{2} & 1/\sqrt{2} & 1/\sqrt{2}\end{bmatrix} \tag{3}$$

$$\boldsymbol{x}_y=x_{yd}+jx_{yq} \tag{4}$$

where $\mathbf{x}_{yabc}=[x_{ya}\ \ x_{yb}\ \ x_{yc}]^T$.

After obtaining the averaged circuit equations and applying the vector DQ transform, one can obtain the converter equations as follows

$$\boldsymbol{v}_s-\boldsymbol{v}_t=r\boldsymbol{i}_L+L\frac{d}{dt}\boldsymbol{i}_L+j\omega L\boldsymbol{i}_L \tag{5}$$

$$C\frac{d}{dt}\boldsymbol{v}_o+j\omega C\boldsymbol{v}_o+\frac{1}{R}\boldsymbol{v}_o=\boldsymbol{i}_s \tag{6}$$

$$\boldsymbol{i}_g=(1-d)\,\boldsymbol{i}_L \tag{7}$$

$$\boldsymbol{v}_t=(1-d)\,\boldsymbol{v}_o \tag{8}$$

where $\boldsymbol{v}_s=v_{sd}+jv_{sq}=V_s$.

In (5) and (6), the term $j\omega L(j\omega C)$ does not mean conventional impedance(admittance) but an element that represents the cross coupling relationship between real part(d-component) equation and imaginary part (q-component) equation. Note that in (5) to (8) all the voltages and current can be regarded as a complex variable which is a function of time.

By using the vector DQ transformed equations of (5) through (8), the vector DQ transformed equivalent circuit can be drawn as shown in Fig. 3.

It should be noted that the equivalent circuit of Fig. 3 possesses the exact information on the presented system, which means, there is no loss in system information in the way of inducing the equivalent.

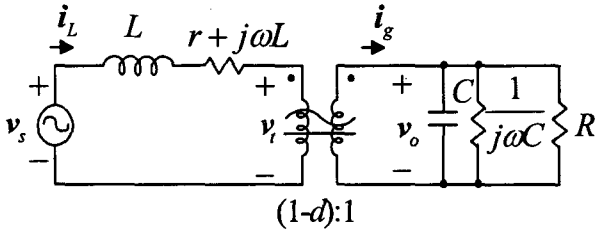

Fig. 3 Vector DQ transformed equivalent circuit

3.2 Steady State Operation

The steady state characteristics can be obtained by considering the DC equivalent circuit as shown in Fig. 4. In steady state operation, the inductors seem to be short and capacitors open when referring to Fig. 3 because all of the DC circuit variables imply DC values.

The steady state operating equations are

$$V_s-(1-D)\,V_o=I_L\,(r+j\omega L) \tag{9}$$

$$(1-D)\,I_L=\left(j\omega C+\frac{1}{R}\right)V_o\ . \tag{10}$$

For convenience, some values are defined as follows

$$Q_L=\frac{\omega L}{r},\ \ Q_C=\omega CR,\ \ \eta=\frac{r}{R},\ \ D'=1-D\ . \tag{11}$$

The voltage conversion relationship will be

$$\frac{V_o}{V_s}=\frac{1}{D'}\cdot\frac{D'^2}{D'^2+\eta-Q_LQ_C\eta+j(Q_L\eta+Q_C\eta)}=\frac{1}{D'}\cdot\rho\angle\alpha \tag{12}$$

where

$$\rho=\frac{1}{\sqrt{1+\delta_2+\delta_4}},\quad \delta_2=\frac{2\eta}{D'^2}(1-Q_LQ_C)$$
$$\delta_4=\frac{\eta^2}{D'^2}(1+Q_L^2)(1+Q_C^2). \tag{13}$$

Considering the magnitude, voltage gain G_v is found to be

$$G_v=\left|\frac{V_o}{V_s}\right|=\frac{1}{D'}\cdot\rho\ . \tag{14}$$

It is worth noting that in (12), (13) and (14)

1) Voltage gain of the presented three phase PWM AC-AC boost converter is similar to DC-DC converters, but modified by a factor of ρ.

2) Under general operation, the numeric value of the ρ factor is almost unity.

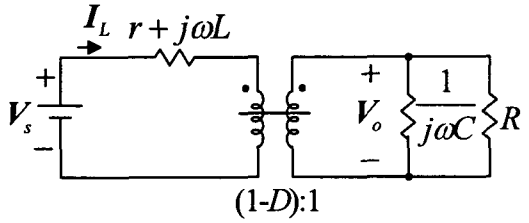

Fig. 4 DC equivalent circuit

3.3 Small Signal Model and Transfer Function

The small signal model is established by introducing some perturbation to the control variable d whereas the input voltage is not perturbed. Then, the circuit variables consist of DC and AC components. The perturbed component is indicated by the diacritical mark '^' of the corresponding variable to distinguish it from the quiescent value denoted by capital letter as follows

$$i_L=I_L+\hat{i}_L,\ v_o=V_o+\hat{v}_o,\ d'=D'-\hat{d}\ . \tag{15}$$

where $d'=1-d$.

Fig. 5 shows the resultant small signal equivalent circuit obtained by applying the perturbation into the vector DQ transformed circuit of Fig. 3. Substituting (15) into (5) to (8), one can obtain

$$\frac{d}{dt}\begin{bmatrix}\hat{v}_o\\ \hat{i}_L\end{bmatrix}=\mathrm{A}\begin{bmatrix}\hat{v}_o\\ \hat{i}_L\end{bmatrix}+\begin{bmatrix}-\frac{I_L}{C}\\ \frac{V_o}{L}\end{bmatrix}\hat{d} \tag{16}$$

where

$$\mathrm{A}=\begin{bmatrix}-j\omega-\frac{1}{RC} & \frac{D'}{C}\\ -\frac{D'}{L} & -j\omega-\frac{r}{L}\end{bmatrix}. \tag{17}$$

Applying Laplace transform to (16) and (17), one can obtain

$$\frac{\hat{v}_o(s)}{\hat{i}_c(s)}=\frac{a-jb}{(sD'CR+2D)+j2D'\omega CR} \tag{18}$$

where $a=\omega^2LCR+D'^2R-rC+sL$, $b=\omega L+\omega rC^2R+s\omega LCR$.

In (18), an assumption is made that the inductor current magnitude perturbation $\hat{i}_L$ is identical to the programmed current command perturbation $\hat{i}_c$. That is $\hat{i}_L(s)\approx\hat{i}_c(s)$. This is valid to the extent that the controller is stable, and that the magnitude of the inductor current ripple is sufficiently small.

From (18), it can be found that the small-signal control-to-output transfer function $\hat{v}_o(s)/\hat{i}_c(s)$ contains only one pole and thus the system order is reduced.

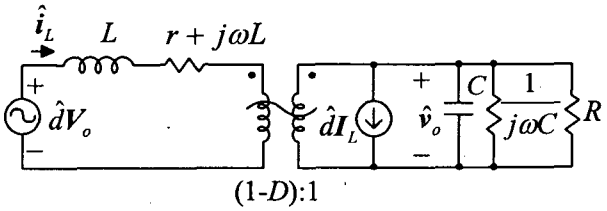

Fig. 5 AC equivalent circuit

4. Experimental Results

To confirm the validity of the design and analysis of the proposed scheme, an experimental setup was made. The circuit parameters are as follows; V_s =110 V, f=60 Hz, L=1.2 mH, r=0.01 Ω, C=20 F, R=30 Ω. Also, the switching frequency is 6 kHz.

With these numeric value substituted into (12) and (13), the conversion ratio can be plotted as a function of the duty ratio with respect to different load resistances. Fig. 6 illustrates the conversion curves with four different load resistances of 5, 10, 15 and 20 Ω. Due to the power circuit energy loss, such as the switches' forward voltage drop and inductor parasitic resistance loss, the maximal voltage gain is limited as shown in Fig. 6.

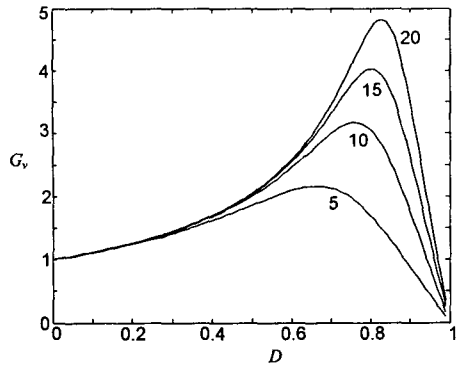

Fig. 6 Voltage gain plot with different load resistances

The described current programmed controller has been implemented using a TMS320F2812 digital signal processor(DSP). Fig. 7 shows the experiment setup of the digitally current programming controlled boost converter. It can be seen in Fig. 7 that except for the sensing circuits, all the controlling behavior is implemented by using DSP, thus fully digital control is realized.

The TMS320F2812 DSP goes still further by providing high speed and high resolution. It offers excellent performance on mathematical calculation and the PWM signal generation, with significant counter programmability and a substantial number of independent PWM channels.

The current control algorithm is implemented by an assembly program, whose flow-chart and is illustrated in Fig. 8. It is worth noting that

1) Due to the high performance of the TMS320F2812 DSP, the execution time of the routines, including analog to digital conversion, is much smaller than the modulation period.

2) The interrupt generated by the period counter, can automatically used to trigger the A/D conversion.

3) Setting the same interrupting frequency with the switching frequency, will make the control variable updated every single switching period.

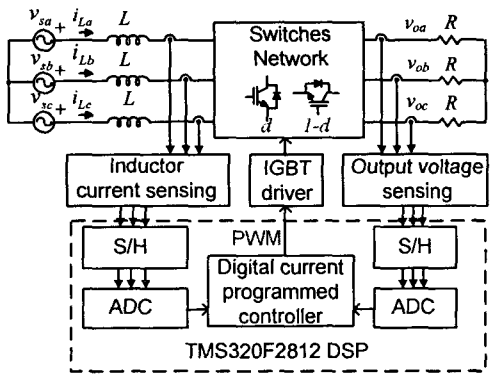

Fig. 7 Experiment setup of the PWM boost converter

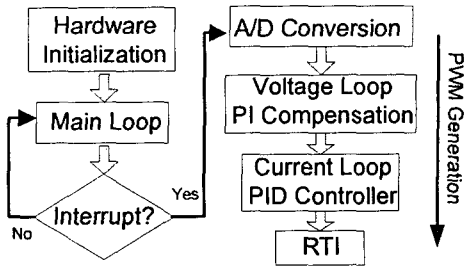

Fig. 8 Flow chart of the control program

Fig. 9 shows the input/output voltage and inductor current waveforms in steady state. In Fig. 9, the output voltage is set to be a magnitude reference of 370 V at peak value. From Fig. 9, it can be seen that the designed current programmed converter operates well in steady state.

Fig. 10 shows the dynamics waveforms of the inductor current, input and output voltage when the peak magnitude voltage reference sets to change from 80V to 240V. It can be seen from Fig. 10 that the output well follows the reference voltage, and the transient time is about one cycle. In Fig. 10, $v_{oab(ext)}$ shows the expanded waveform of v_{oab} around the output voltage reference changing point.

Fig. 11 shows the dynamics waveforms of the input voltage, output voltage and inductor current when the load resistance is set to suffer abrupt change from 30 Ω to 15 Ω. As seen in Fig. 11, the controlled converter employing the digital current mode controller is stable and well operated.

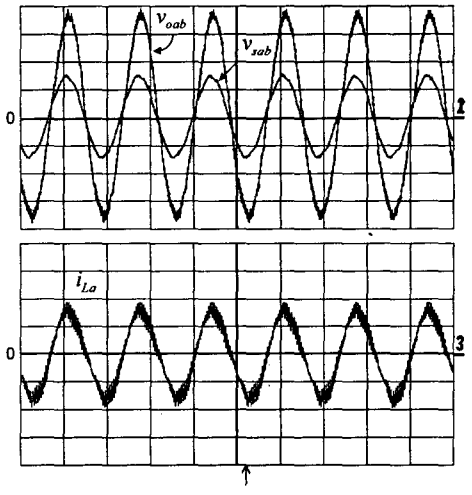

Fig. 9 Steady state operation waveforms: v_{sab}(100V/div, 20ms/div), v_{oab}(100V/div, 20ms/div), i_{La}(20A/div, 20ms/div)

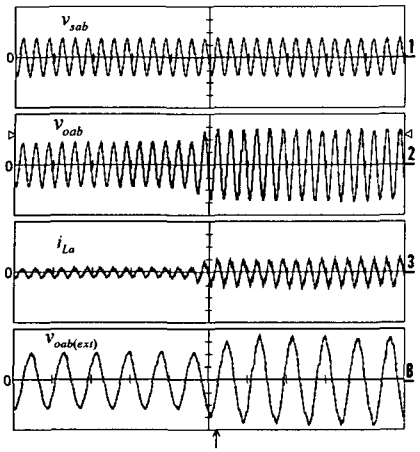

Fig. 10 Dynamics waveforms for voltage reference change; v_{sab}(100V/div, 50ms/div), v_{oab}(100V/div, 50ms/div), i_{La}(20A/div, 50ms/div), $v_{oab(ext)}$(81V/div, 20ms/div)

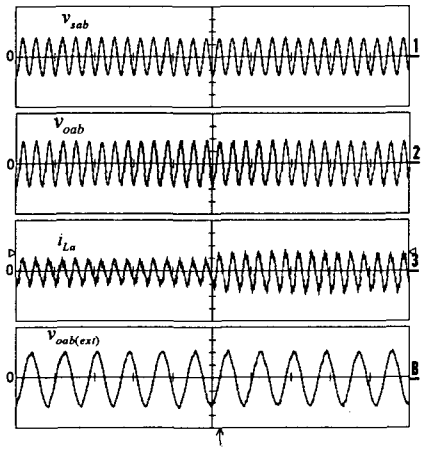

Fig. 11 Dynamics waveforms for load resistance change; v_{sab}(100V/div, 50ms/div), v_{oab}(100V/div, 50ms/div), i_{La}(20A/div, 50ms/div), $v_{oab(ext)}$(81V/div, 20ms/div)

5. Conclusion

This paper deals with the current programmed control of three phase PWM AC-AC boost converter. A similar scheme of DC-DC converter in current programmed mode is extended to AC-AC case by considering the magnitude components. Circuit analysis is carried out by using vector DQ transform method. Small signal model and transfer function are investigated. The experiment results support the validity and feasibility of the design and analysis.

Acknowledgements

This work has been supported by KESRI (R-2003-B-469), which is funded by MOCIE (Ministry of Commerce, Industry and Energy).

References

[1] R. D. Middlebrook, "Modeling Current Programmed Buck and Boost Regulators", IEEE Transactions on Power Electronics, Vol. 4, pp. 36-52, January 1989.

[2] R. D. Middlebrook, "Topics in Multiple-Loop Regulators and Current-Mode Programming", IEEE Power Electronics Specialists Conference Record, pp. 716-732, 1985.

[3] R. Ridley, "A New Continuous-Time Model for Current-Mode Control", IEEE Transactions on Power Electronics, Vol. 6, No. 2, pp. 271-280, April 1991.

[4] F. D. Tan and R. D. Middlebrook, "Unified Modeling and Measurement of Current-Programmed Converters", IEEE Power Electronics Specialists Conference Record, pp. 503-511, 1993.

[5] Kwon, B.-H., Min, B.-D. and Kim, J.-H., "Novel topologies of AC choppers", IEE Proceedings: Electric Power Applications, Volume 143, No. 4, pp. 323-330, 1996.

[6] Soo-Bin Han, Gyu-Hyeong Cho, Bong-Man Jung and Soo-Hyun Choi, "Vector-transformed circuit theory and application to converter modeling/ analysis", Power Electronics Specialists Conference Record, Vol. 1, pp. 538-544, 1998.

저 자 소 개

최 남 섭 (崔 南 燮)

1963년 3월 5일생. 1987년 고려대 전기공학과 졸업. 1989년 KAIST 전기및전자공학과 졸업(석사), 1994년 KAIST 전기및전자공학과 졸업(공박), 1995년~현재 여수대학교 전자통신전기공학부 부교수

Tel : 061-659-3311

E-mail : nschoi@yosu.ac.kr

Li Yulong (李 玉 龍)

1982년 8월 14일생. 2004년 중국 북경석유화공학원 통신공학과 졸업(학사). 2004년~현재 여수대 대학원 전기공학과 석사과정

Tel : 010-2427-1982

E-mail : liyulong@yosu.ac.kr